Available online at www.sciencedirect.com
ScienceDirect
Nuclear Engineering and Design 238 (2008) 1535–1546
Nuclear Engineering and Design
www.elsevier.com/locate/nucengdes

Multiple reheat helium Brayton cycles for sodium cooled fast reactors

Haihua Zhao [a,*], Per F. Peterson [b]

[a] *Idaho National Laboratory, P.O. Box 1625, Idaho Falls, ID 83415-3870, USA*
[b] *Department of Nuclear Engineering, University of California, Berkeley, CA 94720-1730, USA*

Received 30 May 2007; received in revised form 25 November 2007; accepted 5 December 2007

Abstract

Sodium cooled fast reactors (SFR) traditionally adopt the steam Rankine cycle for power conversion. The resulting potential for water–sodium reaction remains a continuing concern which at least partly delays the SFR technology commercialization and is a contributor to higher capital cost. Supercritical CO_2 provides an alternative, but is also capable of sustaining energetic chemical reactions with sodium. Recent development of advanced inert-gas Brayton cycles could potentially solve this compatibility issue, increase thermal efficiency, and bring down the capital cost sufficiently to compete directly with light water reactors. In this paper, helium Brayton cycles with multiple reheat and intercooling states are presented for SFRs with reactor outlet temperatures in the range of 510–650 °C. The resulting thermal efficiencies range from 39% to 47%, which is comparable with supercritical recompression CO_2 cycles (SCO2 cycle). A systematic comparison between the multiple reheat helium Brayton cycle and the SCO2 cycle is given, considering compatibility issues, plant site cooling temperature effect on plant efficiency, full plant cost optimization, and other important factors. The study indicates that the multiple reheat helium cycle is the preferred choice over SCO2 cycle for sodium cooled fast reactors.
Published by Elsevier B.V.

1. Introduction

The sodium cooled fast reactor (SFR) has been studied since the early period of nuclear energy development. Recently the US Global Nuclear Energy Partnership (GNEP) has proposed to use the SFR as an advanced burner reactor (ABR) to close the nuclear fuel cycle (Chang et al., 2006). Although successful operating experience with past and existing test and prototype SFRs has demonstrated generally good safety and reliability of sodium cooled fast reactors, incidents and failures did occur in these prototype reactors and plants (IAEA, 1995). One of major issues that have impeded the commercialization of the SFR is cost. Even advanced SFR designs are anticipated to be some 50% more expensive than the current light water reactors. Both safety and economics are affected by the selection of the power conversion system for SFRs. Traditionally, the steam Rankine cycle has been the only available power conversion choice for SFRs. The potential for energetic water–sodium reactions is a long-standing issue that at least partially delays the near-term commercialization of SFR technology and is one of major contributors for the relatively high overall cost of the SFR. For example, to prevent and mitigate sodium–water reactions in steam generators, expensive double walled tubing and complex safety systems are used. Concern about sodium reactions remains, as sodium leakage incidents have occurred in a majority of the larger prototype SFRs. BN-600 in Russia had 12 sodium leakage incidents during its first 15 years of operation (IAEA, 1995). Therefore advanced SFR designs must address the water–sodium reaction safety concern and improve economics. Advanced closed gas Brayton cycles with compatible fluid such as the inert gas helium provide an opportunity to address this issue.

Gas turbine power conversion systems have become a mature technology due to the large scale deployment of natural gas fired power plants in past two decades. Helium Brayton cycles are chosen as power conversion cycle in Generation IV High Temperature Gas Cooled Reactor (HTGR) designs such as the General Atomics Gas Turbine-Modular Helium Reactor (GT-MHR) (Labar, 2002) and Pebble Bed Modular Reactor (PBMR) (Matzie, 2004). These power conversion systems have undergone detailed engineering design and further R&D efforts, particularly for the PBMR, will solve development issues related to closed gas cycles. Net thermal efficiency in the range of 42%–48% is predicted with turbine inlet temperature from 850 to 900 °C. However, current SFRs can only achieve reactor

* Corresponding author. Tel.: +1 208 526 2679; fax: +1 208 526 0528.
E-mail address: Haihua.Zhao@inl.gov (H. Zhao).

0029-5493/$ – see front matter. Published by Elsevier B.V.
doi:10.1016/j.nucengdes.2007.12.002

outlet temperatures between 500 and 550 °C due to metallic clad peak temperature limit. Even considering longer term advances in materials, the possible reactor outlet temperature may only increase to 650 °C due to the sodium boiling temperature of 881.4 °C. Under this range of reactor outlet temperatures, the conventional closed helium Brayton cycle has significantly lower efficiency than steam cycles. One of solutions to improve the Brayton cycle efficiency can be through multiple reheat and intercooling.

Reheat is not a new concept for power cycles. It is widely used in almost all modern steam cycles. For gas-cooled reactors reheat has not proven to be practicable due to the high pressure loss associated with pumping helium to and from the reactor core. Because molten coolants such as sodium can transport heat with low pumping power to compact heat exchangers, reheat becomes an attractive option with molten coolants. By utilizing reheat, these multiple reheat molten coolant gas cycles (MCGC) have the potential for substantially higher thermal efficiency than current gas cooled reactors, if used with comparable turbine inlet temperatures (Peterson, 2003). MCGC power conversion systems (PCS) using heat from high-temperature liquid salts achieve net thermal efficiencies of 56%, 51%, and 48% for turbine inlet temperatures of 900, 750, and 675 °C, respectively (Zhao and Peterson, 2007). Very high PCS power densities are achieved in these designs, which could imply a large material saving and low construction cost, and bring down the specific PCS cost to about half that of the current GT-MHR PCS design. MCGC designs were also applied for fusion power plant conceptual design (Zhao et al., 2005).

Fig. 1 provides a *T*-s diagram for a low temperature MCGC reference design, which shows the basic idea of MCGC cycle. Using multiple reheat and cooling stages, and recuperation, the overall thermal efficiency can approach Carnot cycle efficiency. With multiple reheat stages, the average heat absorbing temperature is close the highest heat source temperature; with multiple cooling stages, the average heat rejection temperature is close the heat sink temperature. The heat transfer in the recuperator is internal, and does not affect the average heat input and heat rejection temperatures. The cycle efficiency for this optimized reference design shown in this figure is 44% at a turbine inlet temperature of 550 °C (T_a in Fig. 1). For liquid heating sources like sodium, both the pipe diameters and pumping power needed for reheat are much smaller than for gas.

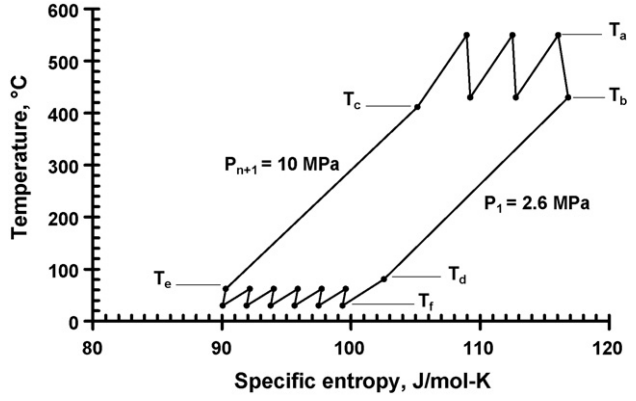

Fig. 1. Temperature-entropy diagram for the MCGC low-temperature reference case. Where T_a is the turbine inlet temperature, T_b the turbine outlet temperature, T_c the recuperator high-pressure side outlet temperature, T_d the recuperator low-pressure side outlet temperature, T_e the compressor outlet temperature, and T_f the compressor inlet temperature.

In this paper, MCGC power conversion system designs for SFRs are presented. Section 2 briefly discusses design assumptions and methods. Section 3 describes power conversion unit (PCU) arrangement. Section 4 presents major design results. Section 5 provides a comprehensive comparison of MCGC with supercritical carbon dioxide cycle (SCO2) (Dostal et al., 2006a,b). SCO2 cycles are recently proposed as power conversion systems by several countries in their advanced sodium fast reactor designs, such as US ABR design (Chang et al., 2006) and Japan (Mito et al., 2006). One of purposes of this paper is to give some insights on systematic comparison of different power conversion systems for SFRs, where multiple reheat helium Brayton cycles enjoy the safety benefit of an inert power cycle working fluid.

2. MCGC design methods, assumptions, and optimization process

2.1. MCGC thermal cycle efficiency calculation

As shown in Fig. 1, for an optimal cycle the multiple-reheat turbines are sized to provide equal pressure expansion ratios. The gas entering each turbine is heated to the same inlet temperature, using the intermediate coolant in a counter-flow heat exchanger. Likewise the compressors are sized to provide equal compression ratios. The gas entering each compressor is cooled to the same temperature, using water in a counter-flow heat exchanger. The original study (Peterson, 2003) provided equations for analyzing the thermal efficiency of the MCGC, which are summarized below.

$$\frac{W_t}{M} = (T_a - T_b) = \eta_t (T_a - T_{bs}) \tag{1}$$

$$\frac{W_c}{M} = (T_e - T_f) = \frac{(T_{es} - T_f)}{\eta_c} \tag{2}$$

where W is the power, M the mass flow rate times specific heat, T absolute temperature, η_t the turbine efficiency, and η_c the compressor efficiency. The definition of T_a, T_b, T_c, T_d, T_e and T_f are shown in Fig. 1. The total pressure ratio for the cycle is then

$$\frac{P_{n+1}}{P_1} = \pi_c \left(\frac{T_{es}}{T_f}\right)^{n\gamma/(\gamma-1)} = \left(\frac{T_a}{T_{bs}}\right)^{m\gamma/(\gamma-1)} \tag{3}$$

where P is pressure, γ the gas constant, assumed to be constant, n the number of compression stages, m the number of expansion stages, and

$$\pi_c = 1 - \frac{\Delta P}{P_{n+1}} \tag{4}$$

corrects for system pressure losses ΔP. Then for specified turbine inlet and outlet temperatures, and compressor inlet

temperature, the compressor outlet temperature T_e can be determined from Eqs. (1–3) as,

$$\frac{P_{n+1}}{P_1} = \pi_c\left(1+\eta_c\left(\frac{T_e}{T_f}-1\right)\right)^{n\gamma/(\gamma-1)} = \left(1-\frac{1}{\eta_t}\left(1-\frac{T_b}{T_a}\right)\right)^{-(m\gamma/(\gamma-1))} \quad (5a)$$

$$T_e = T_f\left\{1+\frac{1}{\eta_c}\left[\pi_c^{-\gamma-1/n\gamma}\left(1-\frac{1}{\eta_t}\left(1-\frac{T_b}{T_a}\right)\right)^{-m/n}-1\right]\right\} \quad (5b)$$

The cycle efficiency η_{MR} can be determined from the heat added Q_H and the net work produced W_n,

$$\frac{Q_H}{M} = m(T_a - T_b) + \Delta T_r \quad (6)$$

$$\frac{W_n}{M} = [m(T_a - T_b) - n(T_e - T_f)] \quad (7)$$

$$\eta_{MR} = \frac{W_n}{Q_H} = \frac{1-(n/m)(T_e-T_f)/(T_a-T_b)}{1+(\Delta T_r/m(T_a-T_b))} \quad (8)$$

$$\eta_{MR} = \frac{W_n}{Q_H} = \frac{1-(T_f/(T_a-T_b)\eta_c)(n/m)[\pi_c^{-((\gamma-1)/n\gamma)}(1-(1/\eta_t)((T_a-T_b)/T_a))^{-m/n}-1]}{1+(\Delta T_r/m(T_a-T_b))} \quad (9)$$

where the average temperature drop across the recuperator ΔT_r is related to the recuperator effectiveness η_r as

$$\Delta T_r = (T_b - T_c) = (T_d - T_e) = (1-\eta_r)(T_b - T_e) \quad (10)$$

As a first order of approximation, one can use the following estimation for the total fractional pressure loss (total pressure loss over system pressure):

$$\pi_c = 1 - (c_r + c_T \cdot m + c_C \cdot n), \quad (11)$$

For the first iteration in solving for cycle efficiency, $c_r = 0.01$ is used for the fractional pressure loss for recuperator, $c_T = 0.01$ fractional pressure loss for one stage of heating and expansion (heater, turbine, and related ducting loss), and $c_C = 0.005$ fractional pressure loss for one stage of cooling and compression (cooler, compressor, and related ducting loss). These parameter values are only used as the initial estimation of system fractional pressure loss. After detailed design for major components such as turbomachinary, heaters, coolers, recuperator, and ducting system is finished, the fractional pressure loss value is updated according to each component's pressure loss.

Using these equations, a parametric search was used to identify promising design parameters under SFR-relevant design constrains.

2.2. Design parameters and assumptions

Two groups of important design parameters affecting cycle efficiency are used to determine the cycle efficiency. The first group is fixed after a reactor design is selected, including

- thermal power 1000 or 2400 MW,
- turbine inlet temperature,
- compressor inlet temperature,
- recuperator effectiveness 0.95,
- compressor efficiency 0.88,
- turbine efficiency 0.93, and
- maximum helium pressure 10 MPa.

The second group is adjustable, including

- numbers of expansion and compression stages,
- turbine outlet temperature or total pressure ratio (defined as the ratio of the maximum pressure over the minimum pressure in the cycle), and
- the system fractional pressure loss coefficient.

The above turbine and compressor efficiencies are adiabatic (or isentropic) efficiencies and the values used are the same as used by the GT-MHR design. Some researchers have used polytropic efficiency and considered real gas effects (Oh and Moore, 2005; Dostal et al., 2006b). The relationship between adiabatic efficiency and polytropic efficiency for a compressor can be expressed as

$$\eta_c = \eta_{poly}\frac{(z-1)(1-(1/\gamma))+1}{z} \quad (12)$$

For turbine the two efficiencies' relationship becomes

$$\eta_t = \eta_{poly}\frac{z}{(z-1)(1-(1/\gamma))+1} \quad (13)$$

where η_c, η_t, and η_{poly} are adiabatic compressor efficiency, adiabatic turbine efficiency, and polytropic efficiency, respectively; z is compressibility factor; and γ is the ratio of specific heat at constant pressure over specific heat at constant volume (5/3 for helium). For helium in the range of consideration, maximum z for the compressor is about 1.06 and maximum z for the turbine is about 1.03. Therefore, the equivalent polytropic efficiency is about 0.91 for compressor and 0.92 for turbine. These equivalent polytropic efficiency values are almost same as used by several recent publications (Oh and Moore, 2005; Dostal et al., 2006b). Because thermal efficiency strongly depends on the assumption of turbomachinery efficiencies, it is important to have consistent turbomachinery efficiency assumptions before comparing different cycle designs. In this paper, only the thermal efficiency (or cycle efficiency used by some authors) is presented in order to more clearly compare different cycles. Net plant efficiency should consider other losses, such as generator efficiency, gearbox or frequency invertor efficiency if used, cooler pumping power, houseload and other consumptions. These values vary with PCS design, component design, plant power level, and

other factors. It is reasonable to assume that the net reduction on efficiency is similar for different cycles.

Turbine inlet and compressor inlet temperatures are chosen according to heat source temperature and heat sink temperature. For sodium fast reactors, the reactor core outlet temperatures currently range from 510 °C for metallic fuel to 550 °C for oxide fuel. Corresponding turbine inlet temperatures at 470 and 520 °C are used for these two SFR designs. A turbine inlet temperature at 550 °C is also included in this paper, which can be taken as a potential value considering near term improvement on SFR design so that reactor outlet temperature can be further increased by 20–40 °C. The fourth case considered is for turbine inlet temperature at 600 °C, this represents the longer term case requiring significant improvement on SFR material and design. The two higher temperature cases can be also directly applied for heavy metal cooled fast reactor designs. The compressor inlet temperature is determined by the specific heat sink and thus varies with plant sites and ambient conditions. Analysis later in this paper shows that heat sink temperature variation has important effect on efficiency. As the reference design choice, 30 °C is chosen as compressor inlet temperature.

Thermal power affects the economics of scale. Larger plants tend to be less expensive in the sense of cost per kWh electricity generation. 1000 MWt is chosen to represent current demonstration SFR plant design such as the Advanced Burner Reactor concept in US (Chang et al., 2006) and 2400 MWt is chosen for near term or long term commercial design to take advantage of economics of scale.

A recuperator effectiveness value at 95% is used by almost all the advanced Brayton cycle designs. Multiple reheat Brayton cycles require smaller recuperators, and are less sensitive to the recuperator effectiveness, than are conventional closed Brayton cycles.

System pressure is a parameter that can be optimized according to cycle design, the state-of-the-art for high-temperature materials subjected to high pressure, and overall cost. Higher pressure can reduce relative pressure loss and increase cycle thermal efficiency. Higher pressure also decreases the component equipment size, such as the heat exchangers, turbomachinery, and gas ducting system. Higher system pressure complicates heater design because the intermediate sodium loop usually has low pressure and the heaters operate under the highest temperature and largest pressure difference in the entire PCS. Higher system pressure may also increase helium leakage. GT-MHR uses a peak pressure of 7.24 MPa and PBMR uses a peak pressure of 9 MPa. The MCGC system is an indirect cycle, with the entire pressure boundary operating at low temperature—the compressor outlet temperature; therefore, it can use higher pressure economically. The current design assumes 10 MPa. Further increase of the system pressure is possible, but detailed economic analysis is needed to choose the optimal pressure.

The second group of parameters such as numbers of expansion and compression stages, turbine outlet temperature and the system fractional pressure loss coefficient, are adjustable. The total pressure ratio can be derived from other parameters if the turbine outlet temperature is chosen as a variable.

2.3. Design methods

A set of design and analysis Mathcad codes were developed to size the major components and analyze the system performance. These include:

- cycle thermal dynamical analysis code—which calculates the thermal efficiency, finds optimal values, and performs sensitivity analysis;
- compact heat exchanger design code—given thermal input data, calculates the total heat transfer area, pressure losses, and selects the heat exchanger module sizes;
- turbomachinery sizing code—estimates the sizes and pressure losses of all the turbines and compressors;
- duct system sizing code—calculates the connection duct size and pressure losses;
- material input code—estimates total helium inventory, total solid material input, and calculate the power density and specific steel input;
- properties database code—contain extensive collections of the solid and fluid physical and transport properties, including helium, sodium, high-temperature alloys used in PCS design.

The cycle thermal dynamics analysis code is developed basing on MCGC analysis equations list from 1 to 10. Input data are based on GT-MHR PCS system parameters and component design results.

The compact heat exchanger design code assumes that all these compact heat exchangers (heaters and recuperator) use offset fin channels to enhance heat transfer. LMTD design procedures (Kays and London, 1984) are used to size heat exchangers and calculate pressure losses. Reference (Manglik and Bergles, 1995) provides heat transfer and pressure loss correlations for offset strip fin channels. Heaters and the recuperator will be made of common high temperature steel such as 316L used for the recuperator in GT-MHR design. All of these compact HX designs use mm scale thick wall and fins to achieve high power density. Similar non-compact type of coolers as used in the 1996 GT-MHR design are also used for the MCGC PCS coolers. The volumes of coolers are calculated using the ratio of thermal power and the GT-MHR cooler volumes.

The turbomachinery sizing code uses simple design methods (Fielding, 2000) to size turbines and compressors and calculate pressure losses. All the turbines and compressors are synchronous (3600 rpm). Also the same dynamic pressure recovery ratios for turbine and compressor exits as GT-MHR are used. The sizes of stators and bearings are estimated according to power scaling from the corresponding GT-MHR designs.

The duct system sizing code calculates the size of connection ducts and pressure losses. All of the form losses and wall friction losses are accounted for in the pressure loss calculation. The total fractional pressure loss for all of the connection ducts is less than 2% of the system total pressure.

The material input code calculates figures of merit such as specific power density, specific steel input, and specific helium inventory. Specific power density is defined as the electrical power per unit of PCS volume. It is an indicator of material con-

sumption and building volume. Specific steel input is defined as the steel mass per unit of electricity power. It is a direct indicator of major material cost for a PCS system. Specific helium inventory is defined as helium mass per unit of electricity power. It decides helium cost and storage volume requirements. Storage is required both for maintenance, and for power control, because power changes are achieved by changing the gas inventory. After sizing of each major component in the PCS, it is relatively straightforward to estimate specific power density and specific helium inventory. It is difficult to precisely account for the total material consumption without a detailed engineering design. However, it is possible to estimate the major material inputs for the PCS by including major PCS components such as the pressure boundary (pressure vessels and ducts), generator, turbomachinery, and heat exchangers. There are two methods to estimate the material mass for components: direct calculation and scaling. For pressure boundary masses, almost all the pressure boundaries are in the form of cylindrical vessels. The wall thickness for a cylinder vessel wall can be estimated using:

$$t = \frac{P \cdot D}{2\sigma_{\text{allowable}}} \tag{14}$$

where t is the vessel thickness, P pressure, D vessel diameter, and $\sigma_{\text{allowable}}$ the allowable stress. Heater and recuperator masses are estimated from component design calculations by assuming materials used. The masses for coolers, generator, and turbomachinery are scaled from GT-MHR design data, according to the following equation:

$$m_{\text{MR}} = m_{\text{GT-MHR}} \frac{Q_{\text{MR}}}{Q_{\text{GT-MHR}}} \tag{15}$$

where m_{MR} is the multiple-reheat cycle component mass, $m_{\text{GT-MHR}}$ the corresponding GT-MHR component mass, Q_{MR} the multiple-reheat cycle component capacity, and $Q_{\text{GT-MHR}}$ the corresponding GT-MHR component capacity.

2.4. Optimization process

The design procedures include the following steps: first the numbers of expansion and compression stages are specified, and then the turbine outlet temperature is selected according to maximum heat source temperature, total pressure ratio, mass flow rate, recuperator power, and, most important—the optimal thermal efficiency. Based on these parameters, each component is designed, such as heaters, turbomachinery, coolers, recuperator and ducts. Finally the system pressure loss is calculated and the design process repeated if there exists large difference between the calculated fractional pressure loss value and the estimated value according to Eq. (11). The following section describes how to select these parameters:

- Select the ratio of expansion stages over compression stages: more stages of compression corresponding to one stage of expansion could increase efficiency. But too many stages of compression result in excessive complexity and cost. As shown in Fig. 2, providing two compression stages for each turbine expansion stage can increase net electricity production by around 2%–5% relative to the case of one compression stage for each expansion stage, depending on the number of expansion stages. However, further increasing compression stages from two to three for each expansion stage produces little or even negative net efficiency gain. Therefore, here two stages of compression are chosen for each stage of expansion, which is also the ratio of compression to expansion stages used in the current GT-MHR and PBMR PCU designs.

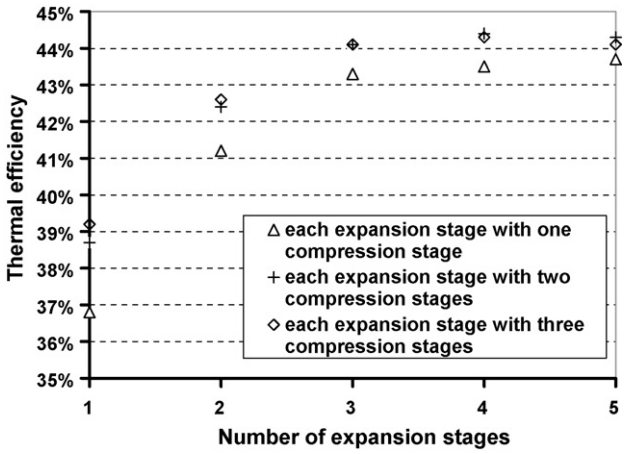

Fig. 2. Optimized thermal efficiency as function of the number of expansion stages and the number of compression stages, for the turbine inlet temperature at 550 °C.

- Select the number of expansion stages: with the ratio of expansion stages over compression stages is determined, the number of expansion stages can be selected. Thermal efficiency increases with the increase of the number of expansion stages until that too many expansion stages result in excessive pressure loss. As shown in Fig. 2, the efficiency gains relative to the one expansion stage case are 9.6%, 14%, 14.7%, and 14.5% for cases with two, three, four, and five expansion stages, respectively. Too many stages of expansion will result in very large total pressure ratio and very complex and expensive ducting systems. A very large pressure ratio will make the recuperator smaller, therefore reduce total heat transfer area and heat exchanger cost, but will complicate the designs of the recuperator (large pressure difference between hot side and cold side) and low pressure turbines (low power density and large blade diameter), therefore at most 4 stages of expansion is feasible. For most cases, 3 expansion stages may be the best choice with 6 stages of compression.
- Select the turbine outlet temperature: within a range, thermal efficiency is not very sensitive to the turbine outlet temperature. Higher turbine outlet temperature means smaller total pressure ratio. The mass flow rate increases with turbine outlet temperature. A larger mass flow rate requires larger turbomachinery and larger duct diameters. Higher turbine outlet temperature also means larger and more expensive recuperator because turbine outlet temperature affects the choice of the recuperator material. Fig. 3 shows the change of the thermal efficiency with the turbine outlet temperature for different combinations of numbers of expansion stages and compres-

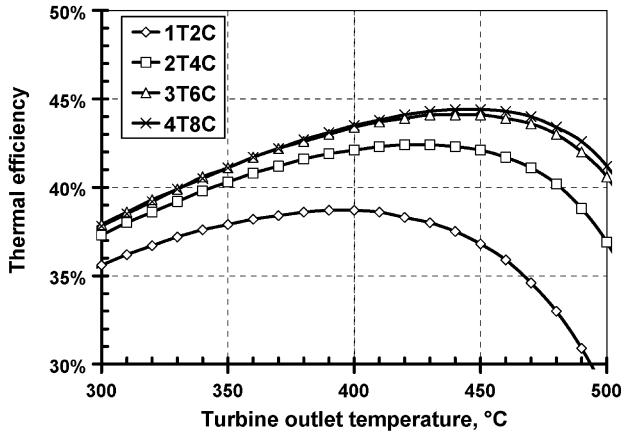

Fig. 3. Thermal efficiency change with the turbine outlet temperature for different configurations, for the turbine inlet temperature at 550 °C. 1T2C: 1 expansion stage and 2 compression stages; 2T4C: 2 expansion stages and 4 compression stages; 3T6C: three expansion stages and 6 compression stages; 4T8C: four expansion stages and 8 compression stages.

sion stage. These cases shown in the figure are for the cycles with the turbine inlet temperature at 550 °C.

More detailed description of PCS designs can be found in previous publications (Zhao and Peterson, 2006, 2007).

3. MCGC PCU arrangement

There are several major equipment design choices to make when considering multiple-reheat Brayton power conversion systems such as: horizontal shaft versus vertical shaft, single shaft versus multiple shafts, and integrated versus distributed equipment configurations. Previous studies (Zhao and Peterson, 2006, 2007) have generated several options for PCU arrangements. Only two designs are summarized here.

Fig. 4 shows the schematics of an integrated vertical multiple-shaft system design which can be derived from GT-MHR PCU design. With relatively small engineering modifications, multiple GT-MHR PCU's can be connected together to create a multiple-reheat cycle power conversion system. The resulting power conversion system is very compact, and results in what is likely the minimum helium duct volume possible for a multiple-reheat system. To do this, compact plate type sodium-to-helium heat exchangers are inserted in the annular space around the turbines, currently occupied by the upper set of recuperator heat exchangers in the GT-MHR design, and the recuperator is moved to a separate pressure vessel. Locating heaters in annular arrangement around turbines gives very short hot-gas flow path.

The left-bottom picture in Fig. 5 shows hot and cold leg configurations for the reference multiple-reheat cycle using three PCU modules (high pressure (HP), middle pressure (MP), and low pressure (LP)) and a separate recuperator vessel (R). An upper hot leg and a lower cold leg connect each pair of PCUs. A separate recuperator vessel is also connected to the low-pressure and high-pressure PCU's with similar hot and cold legs. As shown in Fig. 4, the hot legs connect the PCU vessels at the elevation of the turbine outlets. Flow is collected from the turbine outlet diffuser and crosses the hot leg to the next PCU vessel. This hot-leg flow enters the top of an annular ring of compact heat exchangers and flows downward, to be heated to turbine inlet temperature, and then is ducted directly into the next turbine inlet, resulting in a very short hot-gas flow path. Calculations for the frontal area, flow path length, and volume of these heaters indicate that they can fit without problems in the annular volume around the turbine, currently occupied by the upper recuperator bank of the current GT-MHR PCU design. Likewise, the cold legs connect the PCU's at the elevation of the compressor outlets. Flow is collected from the compressor diffuser, and approximately 90% of the flow crosses the cold leg, and enters the top of an annular ring of coolers to flow downward, to be cooled and then go directly into the next compressor inlet. Approximately 10% of the cold flow is bypassed upward to flow through an annulus around the hot-leg duct, so the hot-leg pressure boundary is maintained at the same temperature as the cold-leg boundary to minimize thermal stresses due to the PCU vessels being connected at two elevations by cross-over legs. The cold cross-over leg eliminates the vessel volume and pressure drop that would be required to bring 100% of the cold flow to the hot-leg elevation to flow across in an annular duct, as is done with direct-cycle gas-cooled reactors. With this config-

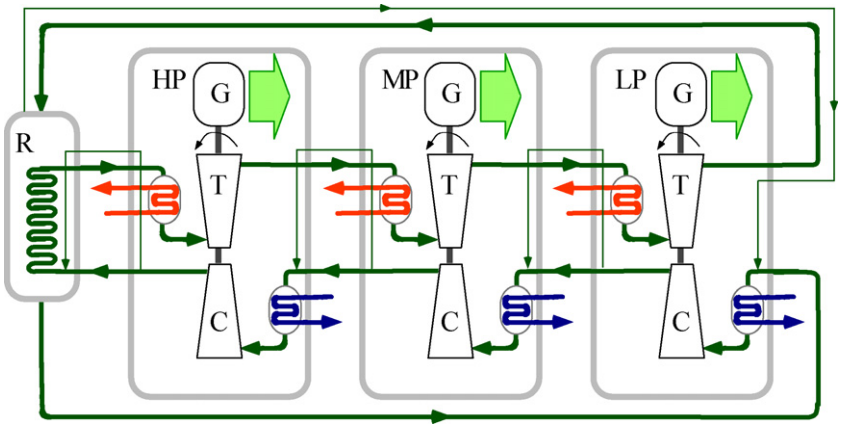

Fig. 4. Schematic flow diagram for the reference three-expansion-stage multiple-reheat cycle, using three PCU modules (HP, MP, and LP) each containing a generator (G), turbine (T), compressor (C), and heater and cooler heat exchangers, with a recuperator (R) located in a fourth vessel.

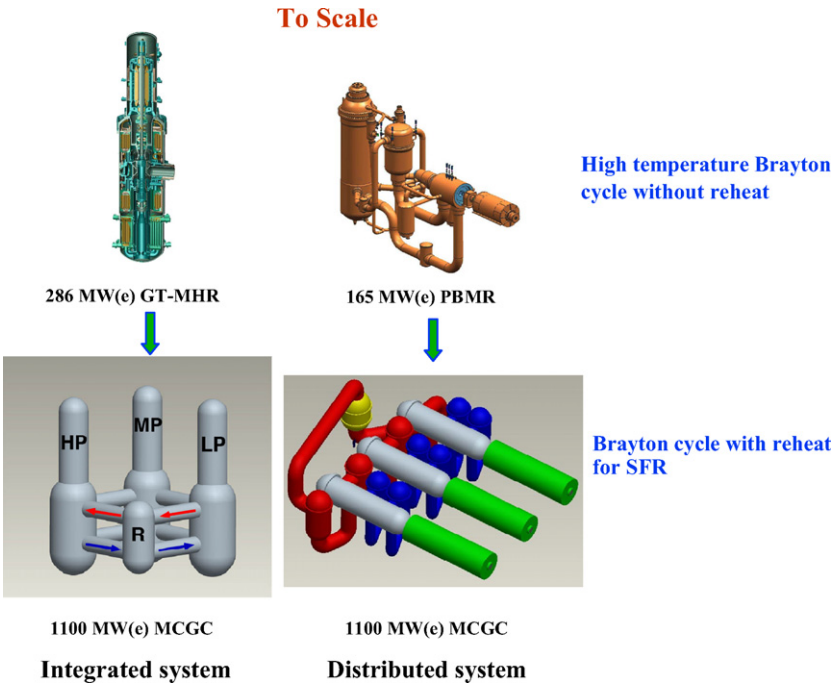

Fig. 5. Scaled comparison of four Brayton power conversion systems. Note the small difference in size between the lower-power (165–286 MW(e)) and high-power (~1100 MW(e)) PCS options.

uration, for the recuperator the low-pressure turbine discharges its gas into a hot leg going over to the top of the recuperator vessel, and the low-pressure gas flows down through the recuperator and then returns to the low-pressure compressor in the low-pressure cold leg. Likewise, the discharge from the high-pressure compressor flows across in the high-pressure cold leg to the recuperator vessel, and flows upward through the recuperator to be heated, and then across in the high-pressure hot leg to the high-pressure PCU.

Fig. 6 shows the schematic flow diagram for the distributed three horizontal-shaft multiple-reheat cycle, using three PCU modules (HP, MP, and LP) each containing a generator, turbine, compressor, and heater and cooler heat exchangers, and a recuperator located in a separate vessel. The counterclockwise flow in the left part of this diagram forms the hot flow loop (not a closed loop, but connected to the cold loop in recuperator), within which high temperature helium flows in heaters, hot ducts, turbines, and the recuperator. The arrangement pattern shown in the diagram is optimized to minimize the total length of hot ducts, which are much more expensive than cold ducts and generate heat losses. All the hot ducts are concentric ducts and cooled by cold helium which flows in the annulus outside hot inner ducts. The clockwise flow going through coolers, cold ducts, compressors and cooling paths for hot ducts forms a larger cold loop.

In all these designs, the pressure boundary operates at, or slightly above, the compressor outlet temperature. This is a very low temperature, and thus the pressure boundary can be made from inexpensive materials. There is also a pressure difference between the cold helium next to the pressure boundary and the hot helium in the hot ducts inside, so the hot ducts and turbine casings must operate with some pressure difference and stress too. However, insulation in these systems can allow the hot components to operate closer to the cold temperature than the hot temperature. The steady-state pressure difference between the hot and cold fluids is minimized.

At this stage, it is difficult to select one to be the best potential system to further develop. But if we consider this choice in the context of broader R&D efforts on Brayton cycle for nuclear power conversion, we will have clearer pictures for future directions. Fig. 5 compares four different power conversion systems. The top two, the GT-MHR and PBMR, are middle power level Brayton cycles without reheat. The two in the bottom are an integral vertical shaft configuration and another horizontal distributed shaft configuration that illustrate the change to middle or large power level Brayton cycles with multiple-reheat. While the net power output can potentially increase by a factor of 5–6, the physical size of the systems are not greatly different from the first-generation GT-MHR and PBMR systems. Multiple reheat Brayton cycles have better efficiency and have the advantage of scaling to high power outputs. Therefore, multiple-reheat Brayton power systems provide a future direction for sodium cooled reactors. In Fig. 5, the systems on the left are vertical shaft and integrated systems; and the systems on the right are horizontal shaft and distributed systems. The success of the GT-MHR, and/or PBMR, program will solve most technology challenges for the development of multiple-reheat systems and will establish the technology base to choose directions for larger multi-reheat systems.

4. MCGC Point design results for SFR

Table 1 summarizes the power conversion design parameters for four peak temperature options and the reference GT-MHR

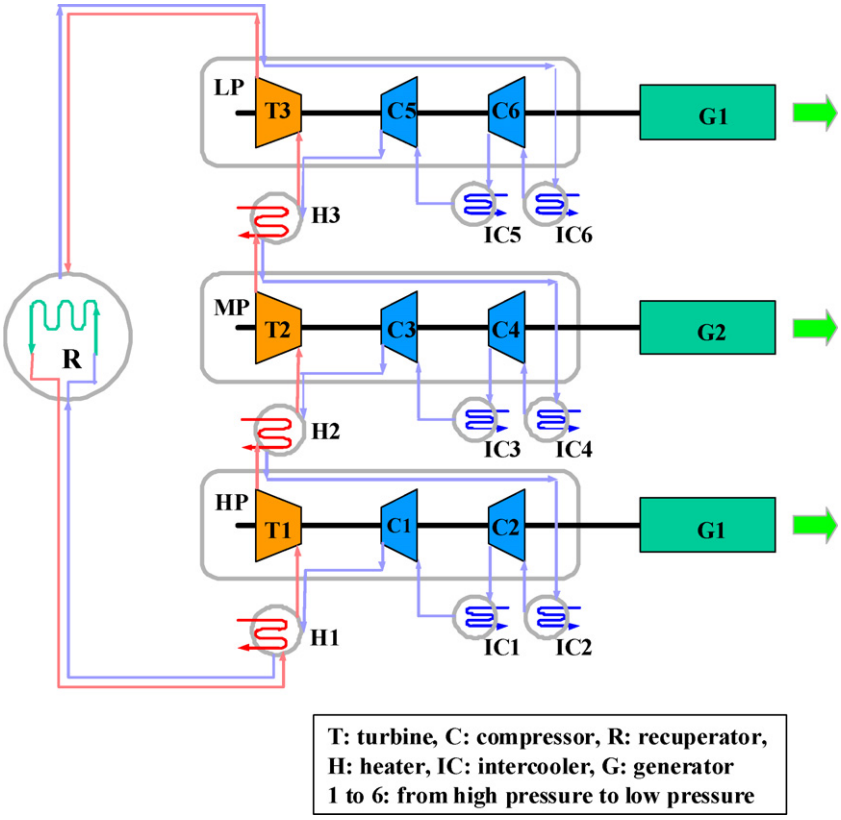

Fig. 6. Schematic flow diagram for the distributed three horizontal-shaft multiple-reheat cycle, using three PCU modules.

Table 1
SFR MCGC system design parameters and comparison with the GT-MHR PCU

	ABR	SFR-oxide	SFR near term	SFR long term	GT-MHR
Thermal power (MW)	1000	1000	2400	2400	600
Primary max./min. temperature (°C)	510/395	550/430	580/455	630/490	848/488
Intermediate max./min. temperature (°C)	480/385	530/420	560/445	610/480	N/A
Turbine inlet/outlet temperature (°C)	470/375	520/410	550/435	600/470	848/508
Compressor inlet/outlet temperature (°C)	30/58	30/60.5	30/60.8	30/63.0	26.4/110.3
System pressure (MPa)	10	10	10	10	7.24
Number of PCU's	3	3	3	3	1
Numbers of turbines and compressors	3/6	3/6	3/6	3/6	1/2
Helium mass flow rate (kg/s)	640	554	1271	1126	317
Cycle pressure ratio (−)	3.03	3.36	3.39	3.70	2.69
Pressure loss fraction (−)	0.06	0.06	0.06	0.06	0.07
Thermal efficiency (−)	0.390	0.423	0.441	0.469	0.48
The Ratio of recuperator power over thermal power (−)	1.00	0.955	0.978	0.942	1.04

Table 2
SFR MCGC system size parameters and comparison with GT-MHR PCUs

	ABR	SFR-Oxide	SFR near term	SFR long term	GT-MHR
PCU total height (m)	28	28	34	34	38
Main PCU vessel diameter (m) (HP, MP and LP)	5.4/5.4/6.2	5.3/5.3/6.1	6.9/6.9/7.8	6.8/6.8/7.7	7.2
Generator vessel diameter (m)	3.5	3.6	4.5	4.5	4.4
Max. turbine tip diameter (m)	1.90	1.91	2.73	2.74	1.783
Max. compressor tip diameter (m)	1.86	1.86	2.65	2.65	1.684
PCUs power density (kW(e)/m^3)	260	290	340	370	230
Specific metal mass for PCUs (MT/MWe) (capacity factor: 0.9)	9.0	8.0	7.2	6.6	7.5
Specific helium inventory (kg/MWe)	17.4	15.2	12.5	11.1	15.9

design, and Table 2 gives the power conversion design main system sizes, power density, specific metal mass and specific helium mass. All the MCGC cycles use three integrated PCUs with vertical shafts and each has one turbine and two compressors. For turbine inlet temperatures of 470 °C (ABR design adjusted with increased reactor core inlet temperature), 520 °C (oxide fuel, current design), 550 °C (oxide fuel, near term design), and 600 °C (long term design), the thermal efficiencies are 39%, 42%, 44%, and 47%, respectively; the corresponding PCU power densities are 260 kW(e)/m^3, 290 kW(e)/m^3, 340 kW(e)/m^3, and 370 kW(e)/m^3, respectively; and the corresponding specific metal masses are 9.0 MT/MWe, 8.0 MT/MWe, 7.2 MT/MWe, and 6.6 MT/MWe, respectively. Note that the first two designs are for middle power demonstration size SFRs (1000 MWt) and the later two designs are for large commercial size SFRs (2400 MWt).

The PCUs power density directly determines structure and building size, therefore the material and construction costs. MCGC systems shown in Table 2 have higher power density than GT-MHR PCU system, even though they operate with SFR-relevant temperatures. The higher power densities for MCGC systems are achievable for several reasons: higher system pressure, larger power, and a more compact and shorter helium flow path arrangement. The MCGC systems have similar or smaller PCU vessel diameters as GT-MHR and the MCGC PCU vessels are shorter than GT-MHR PCU vessel. The MCGC turbines and compressors are slightly larger than GT-MHR due to larger mass flow rate. The large MCGC PCS systems for the near term and long term commercial SFR designs have much higher power densities than the GT-MHR PCS, which implies large potential capital savings on PCS building and construction costs relative to GT-MHR PCS.

Besides power density, metal mass per unit electricity output for PCS is another important indicator for equipment cost. For PCUs, most of the metal used is steel. As shown in Table 2, large MCGC PCUs for near and long term commercial SFRs use much less metal per unit electricity output than smaller MCGC PCUs for middle size demonstration SFRs. This is due to economics of scale and improved thermal efficiency. Large MCGC PCUs require similar or less metal per unit electricity output to construct than GT-MHR PCU does. This may imply a significant capital cost saving for large MCGC PCUs systems relative to GT-MHR PCU, due to several reasons: MCGC systems operate under lower temperature and hence can use lower cost metals; MCGC is an indirect cycle and GT-MHR is direct cycle, and the same material for the nuclear island usually costs substantially more than a balance-of-plant application. Large MCGC systems also need less helium mass per MWe than GT-MHR. This will reduce the cost of helium storage and helium cleaning system.

5. Comparison between MCGC and SCO2 recompression Brayton cycles

This section compares MCGC and SCO2 Brayton cycles for SFRs from several aspects. Although supercritical steam cycles may have slightly higher thermal efficiency than SCO2 and MCGC cycles up to 550 °C turbine inlet temperatures (Dostal et al., 2006b), the compatibility issue related to sodium–water reaction mentioned in Section 1 makes water a far less desirable power cycle fluid. Fig. 7 compares the thermal efficiencies for three types of cycles in the interested range of turbine inlet temperatures for SFRs. The conventional closed helium Brayton cycle with intercooling has much lower efficiency than the SCO2 cycle in the interested temperature range, which is the reason why the helium Brayton cycle was not further considered as power conversion choices for SFR in the past. However, when one considers using reheat, the SCO2 cycle only shows slightly better thermal efficiency than MCGC cycle. The difference is so small (maximum efficiency difference is about 1%) that this is within the range of engineering design uncertainty. These efficiency numbers are only for the reference heat sink temperature and for full load. When considering variation of heat sink temperature and operation at partial load, the thermal efficiency shifts to favor the MCGC cycle as shown in the following discussion.

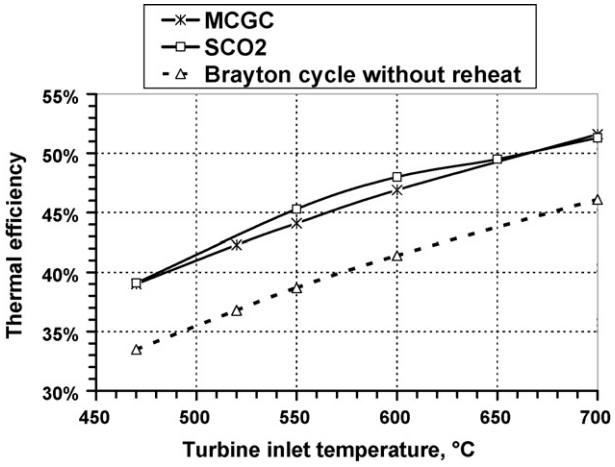

Fig. 7. Comparison of thermal efficiencies of MCGC (3 stages of expansion and 6 stages of compression), SCO2 cycles, and helium Brayton cycle without reheat and with 2 stages of compression.

5.1. Compatibility issue

Power conversion fluid choice is a fundamental issue for SFR plant design. Past experience shows that sodium leakage can occur for large plants within the lifetime of a plant. Heat exchangers between intermediate sodium loop and the power conversion loop have higher potential of leakage due to several reasons: high pressure difference, high operation temperature, large heat transfer area, and thin walls to reduce heat transfer resistance. For a large power plant, the probability of leakage increases approximately proportionally with thermal power. The situation is similar as with PWR plants, in which steam generator tube breaks do occur, and the plant must be shut down for plugging of the failed tube. For leakage in a sodium steam generator, the situation is totally different due to the potential for a violent heat-release reaction between sodium and water. To mitigate the severity of water leaking into intermediate sodium loop, very complex systems must be used as shown in Japan prototype SFR MONJO plant (Matsuura et al., 2007). The safe

systems dealing with sodium–water reaction in sodium steam generator increase the capital cost.

If the SCO2 cycle is adopted for SFR, a similar compatibility problem exists between sodium and CO2 (Choi et al., 2006; Mito et al., 2006) as with water. The energetic reaction of CO_2 with sodium may generate even higher temperatures than sodium–water reactions and the major products include CO and the molten salt of Na_2CO_2. CO gas is toxic, which may threaten the safety of plant workers; Na_2CO_2 may blocks pipes and contaminate the IHX. If a large amount of sodium reacts with CO_2, the released energy may threat the integrity of primary loop. Due to the more severe nature of the Na–CO_2 reaction, it can be anticipated that more expensive and complex safety systems may be required, which may significantly increase the capital cost.

Compared to water and SCO2, helium leakage into intermediate sodium loop has no safety implication for the plant and has very little effect on plant availability. The MCGC can operate at much lower pressure (10 MPa versus 20 MPa for SCO2 cycle), which means a much smaller pressure difference across heaters, and helium is inert gas and does not corrode structure materials while both water and CO_2 are corrosive at high temperature. Therefore, the possibility of heat exchanger wall breaks should be much lower for helium. If any wall break does occur, the break area will not increase due to heating from Na–H_2O or Na–CO_2 reactions. The leaked helium can be recovered in the expansion tank of the intermediate heat transfer loop. The plant can continue to operate unless the break area becomes too large.

5.2. Efficiency in real environments

SCO2 Brayton cycles take advantage of the unique feature of compression work minimized around CO_2 critical point (32 °C, 7 MPa). This brings high efficiency of SCO2 cycle. However, this also brings a substantive disadvantage of SCO2 cycle. Because the SCO2 cycle must be optimized around the critical point for compressor design, any deviation from this point will strongly affect the efficiency. When the compressor inlet temperature increases from 32 to 50 °C, the cycle efficiency will decrease at a rate about 0.28%/°C; when the compressor inlet temperature decreases, the cycle efficiency keeps same or slightly decrease (Dostal et al., 2006a). The MCGC cycle efficiency decreases at a much slower rate, between 0.15% and 0.18%/°C, depending on turbine inlet temperatures, as shown in Fig. 8. The compressor inlet temperature is directly related to the heat sink temperature, which varies on plant location and varies every hour with weather. For example, if dry cooling is used, the heat sink temperature is the atmosphere temperature.

Taking INL (Idaho Falls, ID, USA) as an example of a cold location, the monthly average temperature varies from −7 °C in January to 21 °C in July (according to http://www.accurateweather.com). Assuming that 20 °C temperature difference is needed to remove heat from coolers to atmosphere, Fig. 9 shows the weather-adjusted efficiencies comparison between MCGC and SCO2 cycles. MCGC or simple helium cycles can enjoy the cold winter weather to increase efficiency and subject to weaker penalty on efficiency in summer.

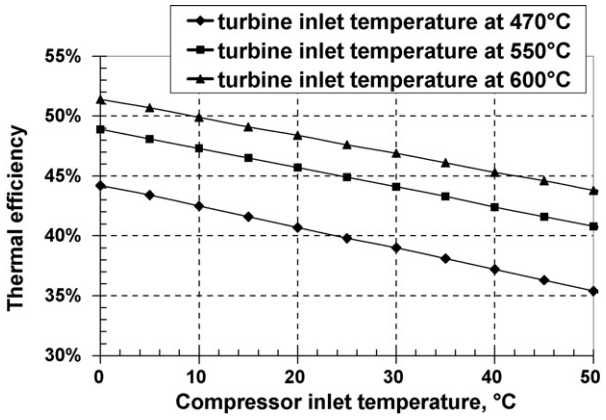

Fig. 8. MCGC thermal efficiencies change with the compressor inlet temperatures.

SCO2 cycle can only keep the optimized efficiency during colder weather and its efficiency decreases more in hotter weather because it is optimized around the 32 °C critical point. The final result is the average efficiency for the MCGC now is 40.8% and for SCO2 is 38.6%. Taking Phoenix, AZ, USA as an example of a hot location, the annually averaged thermal efficiency is 36.6% for MCGC versus 35.9% for SCO2. For 550 °C turbine inlet temperature cases, for both locations, the weather-adjusted average efficiencies are almost same for both types of cycles as shown in Table 3. The above analysis assumes the efficiency can remain at the optimal value when compressor inlet temperature changes. This is not strictly true. However, the SCO2 cycle will subject much stronger penalty on efficiency than helium Brayton cycles because SCO2 cycle is optimized around the critical point and the optimal flow split ratio. For MCGC cycles, when compressor inlet temperature changes, the pressure ratios for turbines and compressors almost keep same; therefore, both turbine and compressor can operate at the optimal efficiency. Extremely hot weather usually means electricity demand peaking, when SCO2 cycles depart from their optimal design conditions most.

When we consider plant locations, such as coastal areas with excellent low temperature seawater heat sink, helium cycles can increase efficiency rapidly while SCO2 cycles have difficulty to benefit; in hot areas, SCO2 cycles will have greater

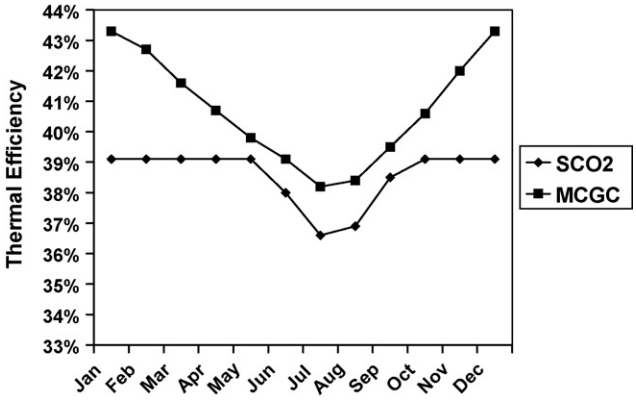

Fig. 9. Weather-adjusted efficiencies comparison between MCGC and SCO2 cycles for the turbine inlet temperature at 470 °C, sited at INL.

Table 3
Comparison of weather-adjusted thermal efficiency for MCGC and SCO2 cycles

Cycle Types	ABR			SFR-near term		
	Reference location	INL	Phoenix	Reference location	INL	Phoenix
SCO2	0.391	0.386	0.359	0.453	0.448	0.421
MCGC	0.390	0.408	0.366	0.441	0.446	0.420

efficiency decrease due to their high sensitivity to compressor inlet temperature. SCO2 cycles can achieve their optimal efficiency only when the cooling temperature varies inside a narrow range. Although simplified, the above analysis clearly shows the importance of site selection on the evaluation of plant efficiency.

5.3. Optimization of PCS and overall plant cost

The PCS cost accounts for 30%–40% of total equipment cost in LWRs (Bryan and Dudley, 1974). However, this ratio is much lower for current SFR plant designs with steam cycles. Current SFRs are more expensive than LWRs, even for SFRs using similar turbine plants. If we assume that turbine plant equipment cost is 30% of total plant equipment cost, that the SFR equipment cost is 1.5 times that of LWR equipment, and that the SFR uses the same turbine equipment as LWR, it is straightforward to estimate that turbine plant equipment for SFR only accounts for about 20% of total plant cost. This conclusion is consistent with the study by MIT (Dostal et al., 2006b). We can compare this with fusion plant design where fusion chamber and related structures and equipments are much more expensive than balance of plant equipment. In terms of optimization of PCS, we can try to increase the efficiency and availability of PCS without worrying too much on PCS cost increase.

Due to higher power density and elimination of huge equipment items like condensers which operate under sub-atmosphere pressure in steam cycles, the Brayton cycle PCS tends to be much smaller and more compact than steam cycles (Peterson and Zhao, 2004). Therefore, the cost ratio of Brayton cycle PCS in total SFR plant can be expected to drop further to the range of 10%–20%. SCO2 cycles have higher power density therefore potential lower cost. However, due to the small portion of PCS in total SFR plant cost, the factor becomes much less important when selecting cycle types. More import factors should be thermal efficiency, long term reliability, and cost and safety effects on reactor system design.

5.4. Other issues

Besides the important factors discussed above, there are many other aspects need to be considered to compare different power cycles, such as partial load efficiency, technical risk, ability to scale up to higher power levels. SCO2 cycles have difficulty to achieve high partial load efficiency. One of possible methods is bypass control scheme, which exhibits an almost linear efficiency decrease with decreasing power (Dostal et al., 2006a). For helium Brayton cycles, helium inventory control can effectively reduce power without affecting the efficiency across a very large power range (General Atomics, 1996). PBMR and GT-MHR have been under detailed engineered design. A PBMR demonstration plant will begin construction in South Africa in 2008. The experience obtained from these design and construction projects can greatly help to develop MCGC cycles.

6. Conclusions

Helium Brayton cycles with multiple reheat and intercooling for SFRs with reactor outlet temperature in the range of 510–650 °C can achieve thermal efficiencies between 39% and 47%, which are comparable with supercritical recompression CO_2 cycles. After a systematic comparison between multiple reheat helium Brayton cycle and the SCO2 cycle, considering the coolant compatibility issue, plant site climate effect on plant efficiency, whole plant cost optimization, and other important factors, it can be concluded that the multiple reheat helium cycle provides excellent characteristics for application to sodium fast reactors.

Acknowledgements

This work was supported through the INL Laboratory Directed Research and Development Program under US DOE Idaho Operations Office Contract DE-AC07-05ID14517.

References

Bryan, R. H., I. T. Dudley. 1974. Estimated Quantities of Materials Contained in a 1000-MW(e) PWR Power Plant, ORNL-TM-4515. Oak Ridge National Laboratory, prepared for the U.S. Atomic Energy Commission.

Chang, Y. I., et al., 2006. Advanced Burner Test Reactor Preconceptual Design Report, ANL-ABR-1 (ANL-AFCI-173), September, 5th, Argonne National Laboratory, USA.

Choi, J. H., et al., 2006. Capsule Test for Investigating Sodium–Carbon Dioxide Interaction, Proceedings of ICAPP '06, Reno, NV USA, June 4-8, Paper 6369.

Dostal, V., Hejzlar, P., Driscoll, M.J., 2006a. High performance supercritical carbon dioxide cycle for next-generation nuclear reactors. Nucl. Technol. 154, 265–282.

Dostal, V., Hejzlar, P., Driscoll, M.J., 2006b. The supercritical carbon dioxide power cycle: comparison with other advanced power cycles. Nucl. Technol. 154, 283–301.

Fielding, L., 2000. Turbine Design: the Effect on Axial Flow Turbine Performance of Parameter Variation. ASME Press.

General Atomics, 1996. GT-MHR Conceptual Design Description Report, GA report No. 7658, July.

IAEA-TECDOC-907, 1995. Conceptual Designs of Advanced Fast Reactors, Technical committee meeting, October 3–6, Kalpakkam, India.

Kays, W.M., London, A.L., 1984. Compact Heat Exchangers, 3rd ed. McGraw-Hill Book Company.

Labar, M.P., 2002. The gas turbine-modular helium reactor: a promising option for near term deployment. In: Proceedings of the 2002 International Congress on Advanced Nuclear Power Plants (ICAPP '02), Embedded Topical American Nuclear Society 2002 Annual Meeting, June 9–13, Hollywood, Florida, USA.

Manglik, R.M., Bergles, A.E., 1995. Heat transfer and pressure drop correlations for the rectangular offset strip fin compact heat exchanger. Exp. Therm. Fluid Sci. 10, 171–180.

Matsuura, M., et al., 2007. Design and Modification of Steam Generator Safety System of FBR MONJU. Nucl. Engn. Des. 237, 1419–1428.

Matzie, R.A., 2004. Pebble bed modular reactor (PBMR) project update. In: Proceeding of the 2004 International Congress on Advances in Nuclear Power Plants (ICAPP '04), Embedded International Topical Meeting 2004 American Nuclear Society Annual Meeting, June 13–17, Pittsburg, Pennsylvania, USA.

Mito, M., et al., 2006. Fast reactor with indirect cycle system of supercritical CO_2 gas turbine plant. In: Proceedings of 2006 International Congress on Advances in Nuclear Power Plants (ICAPP '06), Embedded International Topical Meeting 2006, American Nuclear Society Annual Meeting, June 4-6, Reno, NV, USA.

Oh, C.H., Moore, R.L., 2005. Brayton cycle for high-temperature gas-cooled reactors. Nucl. Technol. 149, 324–336.

Peterson, P.F., 2003. Multiple-reheat Brayton cycles for nuclear power conversion with molten coolants. Nucl. Technol. 144, 279–288.

Peterson, P.F., Zhao, H., 2004. Material input for advanced Brayton cycle power conversion systems. Trans. Am. Nucl. Soc. 91, 420–421.

Zhao, H., Fukuda, G., Abbott, R., Peterson, P.F., 2005. Optimized helium–Brayton power conversion for fusion energy systems. Fusion Sci. Technol. 47, 460–466.

Zhao, H., Peterson, P.F., 2006. Low-temperature multiple-reheat closed gas power cycles for the AHTR and LSFR. In: Proceeding of the 2006 International Congress on Advances in Nuclear Power Plants (ICAPP '06), Embedded International Topical Meeting 2006 American Nuclear Society Annual Meeting, Reno, NV, USA, June 4–6.

Zhao, H., Peterson, P.F., 2007. Optimization of advanced high-temperature Brayton cycles with multiple reheat stages. Nucl. Technol. 158, 145–157.